Self-destruction and dewetting of thin polymer films: the role of interfacial tensions

2003 J. Phys.: Condens. Matter 15 S331

(http://iopscience.iop.org/0953-8984/15/1/345)

INSTITUTE OF PHYSICS PUBLISHING JOURNAL OF PHYSICS: CONDENSED MATTER

J. Phys.: Condens. Matter **15** (2003) S331–S336 PII: S0953-8984(03)55156-6

Self-destruction and dewetting of thin polymer films: the role of interfacial tensions

Günter Reiter[1,3], **Rajesh Khanna**[1,4] **and Ashutosh Sharma**[2]

[1] Institut de Chimie des Surfaces et Interfaces, CNRS-UHA, 15, rue Jean Starcky, BP 2488, 68057 Mulhouse Cedex, France
[2] Department of Chemical Engineering, Indian Institute of Technology at Kanpur, 208 016, India

E-mail: G.Reiter@uha.fr

Received 23 October 2002
Published 16 December 2002
Online at stacks.iop.org/JPhysCM/15/S331

Abstract

We present real-time optical microscopy observations of the pattern evolution in self-destruction and subsequent dewetting of thin polymer films based on experiments with polydimethylsiloxane films sandwiched between silicon wafers and aqueous surfactant solutions. A clear scenario consisting of four distinct stages has been identified: amplification of surface fluctuations, break-up of the film and formation of holes, growth and coalescence of holes, and droplet formation and ripening. Besides a linear dependence on film viscosity and surface tension, the time τ for film rupture varied significantly with film thickness h ($\tau \sim h^5$), as expected from theory. While the role of long-range forces is dominant only in the first stage, the later stages are controlled by the combination of interfacial tensions resulting in the contact angle characterizing the three-phase contact line. During the first stage, the characteristic distance of the pattern remains constant, represented by a time-independent wavevector. In all subsequent stages, this wavevector decreases with time as a consequence of hole opening, coalescence, and ripening on droplets. The later stages of evolution are a function of the contact angle at the three-phase contact line. Only a clear distinction between stages *before* and *after* film break-up allows a correct interpretation of the observed pattern evolution in unstable thin films.

(Some figures in this article are in colour only in the electronic version)

The destruction and pattern formation in thin fluid films is of central importance in many technological applications as well as in a variety of physical and biological thin-film phenomena. The general contours of the mechanics and thermodynamics of thin-film instability have emerged during the last 50 years [1–9]. Initial surface fluctuations at the

[3] Author to whom any correspondence should be addressed.
[4] Present address: Department of Chemical Engineering, Indian Institute of Technology at New Delhi, 16, India.

0953-8984/03/010331+06$30.00

free surface of an initially rather uniform thin film get amplified spontaneously whenever the second derivative of the excess intermolecular free energy (per unit area) with respect to the local film thickness is negative and their wavelength is larger than a critical wavelength. This amplification eventually leads to the break-up and subsequent dewetting of the underlying substrate in the form of dry patches [1–20].

Theory explaining the intrinsic amplification of surface fluctuations and resulting dewetting is already well advanced [1–9], but experimental verification of the various processes involved is still not yet fully accomplished. A major difficulty arises from the fact that most experiments are dealing with rather thin films which cannot be visualized by fast space-resolving optical techniques like microscopy. Although atomic force microscopy (AFM) allowed us to obtain time-resolved real-space information [13, 14, 17, 19], the data obtained in this way are still rather limited. In particular, it is not easily possible to cover a large range of film thickness due to the enormous differences in the times for rupture.

In the present study, we have circumvented these problems by using systems of low viscosity and extremely low interfacial tension between the film and its environment. Relying on theoretical considerations, we will also show that results for films of different viscosity and in contact with different environments can be superposed on one master curve. In addition, using various substrate coatings, we will discuss the influence of contact angle on dewetting.

The experiments were done on thin (<200 nm) polydimethylsiloxane (PDMS) films sandwiched between variously PDMS-coated silicon wafers and water or an aqueous surfactant solution. This system is a suitable one in which to study the self-destruction of thin polymer films as it provides excellent control over intermolecular interactions and kinetics [16, 21, 23, 24]. Four types of coating were used: two monolayers of reactive (Si–H-terminated) short-or long-chain PDMS (polymer brushes): molecular weight, $M_w = 8.8$ and 78 kg mol^{-1}, respectively; polydispersity, $I < 1.1$; and two irreversibly adsorbed PDMS layers representing 'pseudo-brushes' of PDMS containing a dense part of strongly adsorbed segments and a loose part of dangling ends and tails: $M_w = 38$ kg mol^{-1}, $I = 2.6$ and $M_w = 80$ kg mol^{-1}, $I = 2.1$, respectively. The thickness of the '78k' and '8.8k' brush layers was found to be about 15 and 6 nm, respectively, by ellipsometric measurements [16]. For the '38k' and '80k' adsorbed layers, thicknesses of 6 and 9 nm were measured, respectively. Thin PDMS films of various molecular weights (M_w ranging from 3 to 308 kg mol^{-1}, corresponding to viscosities ranging from 10 to 1000 Pa s) were put on the coated silicon wafers by spin-casting dilute solutions of nonreactive PDMS in heptane. Again, ellipsometry was used to measure the thickness of the PDMS film.

In actual experiments the instability was initiated by putting a small drop ($\sim$10 μl) of water or an aqueous solution containing surfactant L77 (polyalkenoxide-modified heptamethyltrisiloxane) on the PDMS film [16, 21, 23, 24]. Adding surfactants changed only the interfacial tension, thereby changing the length scales and timescales of the evolution, without bringing about any qualitative change in different stages of evolution as compared to the case for films under pure water [23]. Aqueous L77 solutions allowed have convenient timescales and length scales for the break-up of comparatively thick films (about 100 nm), which were required to have sufficient optical contrast especially during the early stages. L77 reduced the interfacial tension by about a hundred times to a very low value of about 0.3 mN m^{-1} from about 38.4 mN m^{-1}, which is the value for pure water[5]. The lowering of the interfacial tension led to a faster amplification of the surface waves and smaller length scales, allowing for good statistical analysis. The spatio-temporal evolution of the instability and the resulting

[5] The interfacial tension was estimated on the basis of surface tension measurements made using a Wilhelmy plate apparatus, contact angle goniometry, and Young's equation.

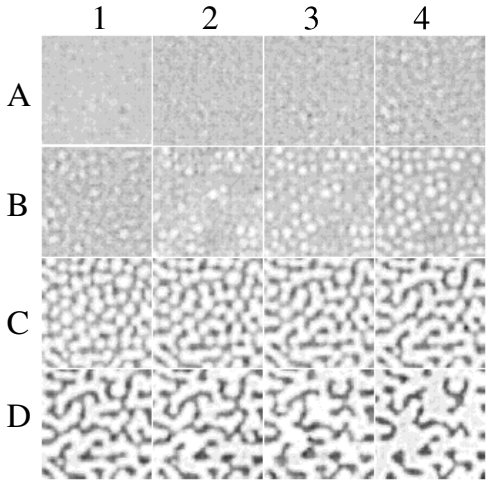

Figure 1. Optical micrographs of evolution of morphological patterns during the self-destruction of a 85 nm thick and highly viscous (1000 Pa s) PDMS film on a silicon wafer coated with a 15 nm thick monolayer of end-grafted PDMS ('78k') molecules. The levels of grey indicate the local thickness of the film, with darker regions representing thicker portions. Different micrographs (from left to right and top to bottom, from A1 to D4) correspond to times (in seconds) of 200, 230, 245, 260, 275, 300, 315, 330, 420, 435, 500, 570, 660, 840, 1110, and 1680, respectively. The area shown in each image is $25 \times 25\ \mu\text{m}^2$.

break-up of the film was observed in real time by optical microscopy and video recorded for later analysis.

Figure 1 presents typical evolution of the morphological pattern during the self-destruction and dewetting of a PDMS film with the help of a time series of optical micrographs.

An undulating pattern emerges from an initially rather smooth film. This low-amplitude pattern amplifies and becomes more pronounced as evolution continues. While the lateral regularity of the structure is maintained during this period, the amplification is nonhomogeneous with different depressions thinning at different rates as indicated by different levels of grey at the different depressions (image A4 of figure 1). This asynchronous formation of holes is expected due to the small differences in the local thickness (reflecting the initial randomly rough surface) which are self-reinforcing at different rates governed by the long-range interactions whose strength increases nonlinearly as the film thins. It can be noted that most of the amplification has occurred in the last 30 s of this stage, which is only about 10% of the total duration of the stage. This also confirms the theoretical predictions [5–9] of the amplification being slow in the beginning—where the surface fluctuations get arranged on a dominant wavelength—but later on entering a nonlinear explosive phase of growth, consistent with an exponential growth of the amplitude.

This amplification of surface fluctuations is followed by the process of 'pseudo-dewetting' initiated by the 'touch-down' of the depressions at the minimum thickness (determined by the grafted or adsorbed layer) to form isolated circular holes (white portions), with the deeper depressions touching earlier (images B1 and B2 in figure 1) and others following later (image B3 in figure 1).

At later stages, as these holes grow in diameter, one can observe coalescence and subsequent droplet formation, followed by some ripening at even longer times. In our system, ripening is facilitated by the underlying PDMS coating connecting the various PDMS droplets.

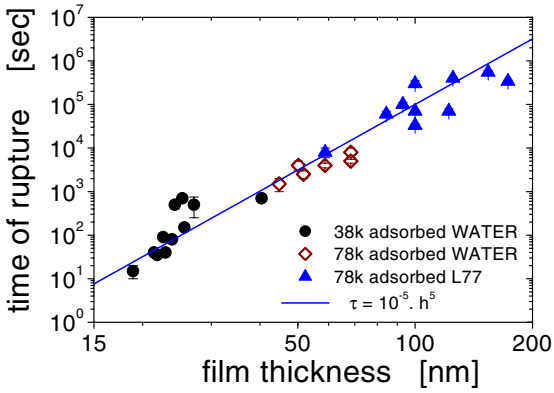

Figure 2. Time τ for film rupture as a function of film thickness h. Circles are for PDMS (1000 Pa s) films on PDMS '38k' adsorbed layers covered by water; diamonds and triangles are for PDMS (viscosity varying between 10 and 1000 Pa s) films on PDMS '78k' grafted layers covered by water and surfactant solution, respectively. All data are normalized to $\eta = 1000$ Pa s and $\gamma = 38.4$ mN m^{-1}.

As shown in figure 1, the time τ of film rupture can be rather precisely determined. On the basis of this procedure we have determined τ for different film thicknesses h, observing a strong increase in τ with h. This increase in τ caused the problem that for thicker films, occasional holes (nucleated by e.g. a defect) had sufficient time to dewet the whole film, excluding the possibility of studying the instability caused by long-range forces. We tried to circumvent this problem by using longer grafted chains which are supposed to slow down dewetting (see later). In addition, we also reduced the viscosity of the film. All data from various systems are presented in figure 2, where we used the linear relationship between τ and viscosity η and γ predicted by theory [1, 3, 4] to superpose data for systems differing in η and γ:

$$\tau \sim \eta\gamma h^5 \tag{1}$$

Although there is significant scatter in the individual data sets, the overall presentation is consistent with $\tau \sim h^5$, as indicated by the full line.

The evolution of patterns like the ones shown in figure 1 can be described by the time dependence of the characteristic wavelength obtained from the position of the peak (q_{max}) of the radially averaged 2D Fourier transforms (figure 3). The superposition of data originating from different systems allows us to distinguish two remarkable features. Before rupture, all systems show that q_{max} stayed constant during the first phase of evolution (compare region A in figure 1). Due to the lack of optical contrast, it is not possible to follow the amplification stage for thin films. Thus, for the high-interfacial-tension 'water system', we cannot determine q_{max} in the early stages.

As expected from theory, for lower γ-values only the absolute value of q_{max} was larger while the value of τ was smaller, allowing us to superpose all data for $t < \tau$. In contrast, at later stages ($t > \tau$), quantitatively different trends for water and surfactant systems were observed, even in the normalized presentation. Hole coalescence, droplet formation, and ripening proceeded much faster when γ was lower. In figure 3, we indicate by multiplying the normalized time by 10 that the process seems to be about a factor of 10 faster. One possible explanation is based on the contact angle (θ) at the three-phase contact line (coated substrate (CS)—PDMS film (PF)—surrounding liquid (SL)) which is significantly higher for the surfactant solution ($\cos\theta = (\gamma_{CS-SL} - \gamma_{CS-PF})/\gamma_{PF-SL}$). The interfacial tension

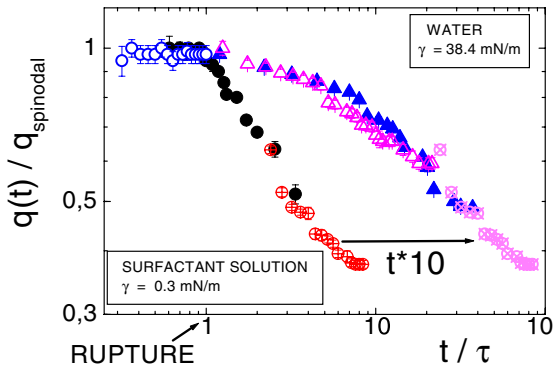

Figure 3. Temporal evolution of the characteristic wavevector $q(t)$ (normalized by its value ($q_{spinodal}$) at times before film rupture) versus time (normalized by the time of rupture τ). All films were on '78k' grafted PDMS layers. Circles and triangles represent films under surfactant solution and water, respectively. The film thickness and viscosity are: 59 nm (10 Pa s) and 35 nm (1 Pa s) for open and full triangles and 125 nm (100 Pa s), 100 nm (1000 Pa s), and 84 nm (100 Pa s) for open, full, and crossed circles, respectively. The last data set has also been replotted at $10t$.

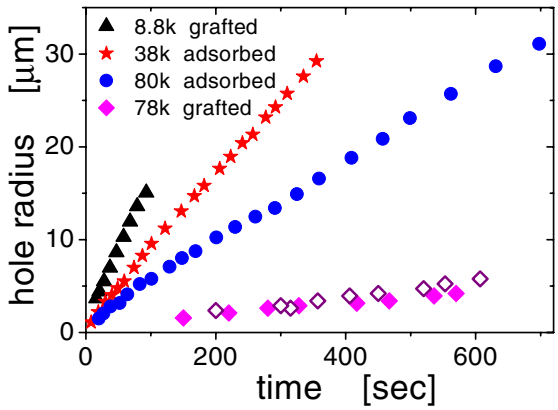

Figure 4. Growth of an isolated hole in about 100 nm thick PDMS films (100 Pa s) on various PDMS coatings as indicated in the key. Open and full diamonds represent two independent measurements of the same type.

between coating and film (γ_{CS-PF}) has not yet been measured for the particular combinations investigated. From comparison with an analogous system [25], we estimate it to be rather small, about 0.1 mN m^{-1}. The interfacial tension between the coating and the SL (γ_{CS-SL}) and between the film and the SL (γ_{PF-SL}) are about the same: 0.3 and 38.4 mN m^{-1} for the surfactant solution and pure water, respectively (see footnote 5). Based on these values and assumptions, we expect for these two cases $\theta \sim 50°$ and 5°, respectively. Thus, significantly different driving forces were pushing at the three-phase contact line for $t > \tau$.

As shown in figure 3, the late stages of film evolution are affected by interfacial tensions represented by the contact angle. In addition, we demonstrate that besides static parameters such as θ, dissipation at the film–coating interface can also affect the temporal evolution of the thin-film pattern. For that purpose, we have looked at the growth of an isolated hole in PDMS films under water, deposited on various PDMS coatings differing mainly in molecular weight and conformational properties and thus providing different friction at the coating–film

interface (figure 4). Assuming that all holes open at constant velocity, we obtained a change by more than one order of magnitude in dewetting velocity V when the molecular weight of the grafted molecules changed from 8.8 to 78 kg mol^{-1}. Consequently, besides θ, interfacial properties also affect V which, in turn, is the parameter controlling hole coalescence and droplet ripening. Thus, besides changing the contact angle (which is supposed to be about the same for all the samples of figure 4), friction at the coating–film interface can control the late stages of pattern formation in thin liquid films.

In summary, we showed that an unstable thin liquid film passes through several stages until it finally reaches equilibrium. The amplification stage is reasonably accurately described by various theoretical works, and was already predicted in a quite correct way by Vrij [1] about 35 years ago. Both film viscosity and the tension at the film–SL interface linearly affect the time needed for rupturing such films. The late stages of pattern formation, however, are dominated by the three-phase contact angle and friction at the coating–film interface.

Acknowledgments

We are indebted to Philippe Auroy for providing us with the end-functionalized PDMS molecules. This work was supported by the Indo-French Centre for the Promotion of Advanced Research/Centre Franco-Indien Pour la Promotion de la Recherche.

References

[1] Vrij A 1966 *Discuss. Faraday Soc.* **42** 23
[2] Williams M B and Davis S H 1982 *J. Colloid Interface Sci.* **90** 220
[3] Brochard-Wyart F and Daillant F 1990 *Can. J. Phys.* **68** 1084
[4] Sharma A 1993 *Langmuir* **9** 861
Sharma A 1993 *Langmuir* **9** 3580
[5] Oron A, Davis S and Bankoff S G 1997 *Rev. Mod. Phys.* **69** 931
[6] Singh J and Sharma A 2000 *J. Adhes. Sci. Technol.* **14** 145
[7] Kargupta K, Konnur R and Sharma A 2001 *Langmuir* **17** 1294
[8] Kargupta K and Sharma A 2002 *J. Colloid Interface Sci.* **245** 99
[9] Bertozzi A L, Grün G and Witelski T P 2001 *Nonlinearity* **14** 1569
[10] Sharma A and Khanna R 1998 *Phys. Rev. Lett.* **81** 3463
[11] Reiter G 1992 *Phys. Rev. Lett.* **68** 75
[12] Sferazza M, Heppenstall-Butler M, Cubitt R and Jones R A L 1998 *Phys. Rev. Lett.* **81** 5173
[13] Xie R *et al* 1998 *Phys. Rev. Lett.* **81** 1251
[14] Herminghaus *et al* 1998 *Science* **282** 916
[15] Thiele U, Mertig M and Pompe W 1998 *Phys. Rev. Lett.* **80** 2869
[16] Reiter G *et al* 1999 *Europhys. Lett.* **46** 512
Reiter G *et al* 1999 *Langmuir* **15** 2551
[17] Segalman R A and Green P F 1999 *Macromolecules* **32** 801
[18] Reiter G 1998 *Science* **282** 888
[19] Seemann R, Herminghaus S and Jacobs K 2001 *Phys. Rev. Lett.* **86** 5534
[20] Higgins A M and Jones R A L 2000 *Nature* **404** 476
[21] Reiter G *et al* 1999 *J. Colloid Interface Sci.* **214** 126
[22] Konnur R, Kargupta K and Sharma A 2000 *Phys. Rev. Lett.* **84** 931
[23] Reiter G, Khanna R and Sharma A 2000 *Phys. Rev. Lett.* **85** 1432
[24] Khanna R, Sharma A and Reiter G 2000 *EPJdirect* E **2** 1 (http://link.springer.de/link/service/journals/10105/bibs/0002001/0002e002/0002e002.htm)
[25] Reiter G and Khanna R 2000 *Phys. Rev. Lett.* **85** 2753
Reiter G and Khanna R 2000 *Langmuir* **16** 6351